

Magnetic coupling in Gd/Ni bilayers

This article has been downloaded from IOPscience. Please scroll down to see the full text article.

2008 J. Phys.: Condens. Matter 20 395232

(<http://iopscience.iop.org/0953-8984/20/39/395232>)

View [the table of contents for this issue](#), or go to the [journal homepage](#) for more

Download details:

IP Address: 129.252.86.83

The article was downloaded on 29/05/2010 at 15:15

Please note that [terms and conditions apply](#).

Magnetic coupling in Gd/Ni bilayers

A Barth¹, F Treubel¹, M Marszałek², W Evenson³, O Hellwig⁴,
C Borschel⁵, M Albrecht¹ and G Schatz¹

¹ Department of Physics, University of Konstanz, D-78457 Konstanz, Germany

² The H Niewodniczanski Institute of Nuclear Physics, Polish Academy of Sciences,
31-348 Kraków, Poland

³ School of Science and Health, Utah State Valley College, Orem, UT 84058, USA

⁴ San Jose Research Center, Hitachi Global Storage Technologies, San Jose, CA 95135, USA

⁵ II Physikalisches Institut, University of Göttingen, D-37077 Göttingen, Germany

E-mail: alexander.barth@uni-konstanz.de

Received 3 March 2008, in final form 1 July 2008

Published 4 September 2008

Online at stacks.iop.org/JPhysCM/20/395232

Abstract

Layered thin films consisting of rare earth materials and magnetic transition metals reveal a variety of magnetic properties due to their complex coupling interactions. The Gd/Ni system adds its own features due to the interplay of saturation moments and Curie temperatures of these two metals. Magnetic coupling in Gd/Ni bilayers leads to negative remanence and interesting magnetic switching behavior, which is strongly temperature-dependent. A transition from the 'nickel-aligned' state to the 'gadolinium-aligned' state is observed at 45 K, independent of the chosen substrate and hence of the Curie point of the Gd layer, which depends on the substrate. In x-ray magnetic circular dichroism experiments a polarization of Gd moments at the interface antiparallel to the Ni layer was observed even at room temperature. Structural analysis show a rough Gd/Ni interface with grains of a few nm and an amorphous Gd growth is indicated by diffraction methods.

1. Introduction

Bilayers present attractive possibilities for designing physical properties by combining two materials with contrasting characteristics. In the case of magnetism, it seems particularly interesting to study bilayer systems composed of magnetic layers with contrasting saturation magnetizations and significantly different Curie temperatures. This can lead to noteworthy effects related to interlayer coupling, including the possibilities of negative remanence and unusual temperature-dependent magnetic reversal mechanisms. Gadolinium and nickel, the subject of this work, are two such contrasting magnetic materials. Gadolinium has a Curie temperature T_C of 293.2 K and a permanent magnetic moment of $7.98 \mu_B$, exceeding, for example, that of nickel ($0.606 \mu_B$ at zero temperature) by a factor of 12. Due to challenging preparation issues associated with handling the rare earths, only a small number of research groups were able to study these materials in the early years. Furthermore, nearly all rare earth elements, if evaporated under UHV conditions, grow non-epitaxially or even in amorphous films; for example, only a few substrates allow epitaxial growth of gadolinium. Gadolinium crystallizes with hcp structure and lattice parameters $a = 0.363$ nm and $c = 0.578$ nm. Nickel,

on the other hand, has an fcc structure with $a = 0.352$ nm and becomes ferromagnetic below $T_C = 627$ K.

Over the last decade, several research groups have studied exchange interactions and magnetic behavior in gadolinium, either as a pure metal or in alloys with other transition metals, including iron, cobalt, CoNi and Permalloy. The coupling of Gd to ferromagnetic materials has been, therefore, a particularly interesting topic of investigation in recent years [1–3], as well as the coupling of magnetic layers through a gadolinium spacer [4–6]. The interaction is still only partially understood because of the complex interaction of the 3d and 4f magnetic moments [7], leading to twisted [8] or even helical spin configurations, as in the case of Dy and Ho [9, 10]. However, systems containing pure nickel layers are hardly discussed in the literature. Possible reasons are the difficulties of determining the interface structure [11], alloying tendencies [4, 5] and the comparatively low Curie temperatures of the GdNi alloys that might be formed [12].

In this study the magnetic interactions between thin gadolinium and nickel layers were investigated, along with their connection to the structural properties of the bilayers. Medium energy electron diffraction (MEED), Auger electron spectroscopy (AES), x-ray diffraction (XRD), Rutherford

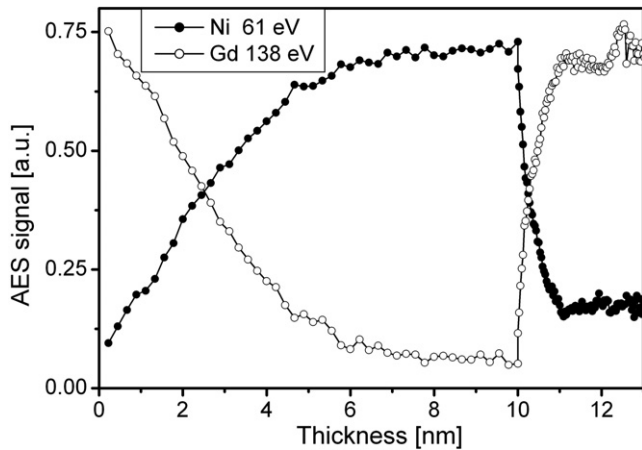


Figure 1. AES signal as a function of Ni thickness. Ni was deposited on a Gd film at $T_{\text{dep}} = 100$ K. At 10 nm Ni thickness deposition was stopped and an additional Gd deposition was started.

backscattering (RBS) and scanning tunneling microscopy (STM) were applied to examine the structural properties on atomic and microscopic scales. The overall magnetic properties of the samples were studied by superconducting quantum interference device (SQUID) magnetometry and element-specific x-ray magnetic circular dichroism (XMCD) performed at the synchrotron BESSY in Berlin.

2. Film preparation and structural characterization

A series of bilayers of Gd and Ni were deposited onto $\text{Al}_2\text{O}_3(0001)$ and Si_3N_4 substrates by molecular beam epitaxy at a deposition temperature of 100 K under a base pressure of 1×10^{-10} mbar. Special care was taken to reduce the amount of oxygen and water in the residual gas. Built-in cooling made it possible to maintain the pressure below 1×10^{-9} mbar during e-beam evaporation, which turned out to be essential for the quality of the Gd layer. All samples consist of a 5.0 nm thick layer of Gd and a 7.5 nm thick layer of Ni. A capping layer of 2.0 nm Au on top, evaporated from a thermal source, protects the bilayer from oxidation. The growth rates were all less than 0.1 nm min^{-1} .

We have applied MEED during growth of the Gd film and observe that MEED reflections from the $\text{Al}_2\text{O}_3(0001)$ substrate already disappear after deposition of 0.2 nm Gd. This suggests that even the first monolayer is amorphous, or nanocrystalline, with a characteristic size smaller than the coherence length of the diffracted electron beam. Amorphous growth of Gd on glass [4, 6, 13], Ni, Ag [4], Cu [14], Si, Si-N and Co [15] has already been reported. Inspection by STM of Gd films on $\text{Al}_2\text{O}_3(0001)$ shows a grainy structure with an average grain size of about 3 nm and a pronounced roughness of the film. In the case of the Si_3N_4 substrate, the grains are larger by about a factor of ten compared to films grown on Al_2O_3 . In addition, we observe significant roughness of the films, which, however, is mainly due to the substrate roughness itself.

Deposition of Ni onto the Gd film which was grown at 100 K on Al_2O_3 was investigated by *in situ* Auger electron spectroscopy. In figure 1, the Ni and Gd signal is recorded as a

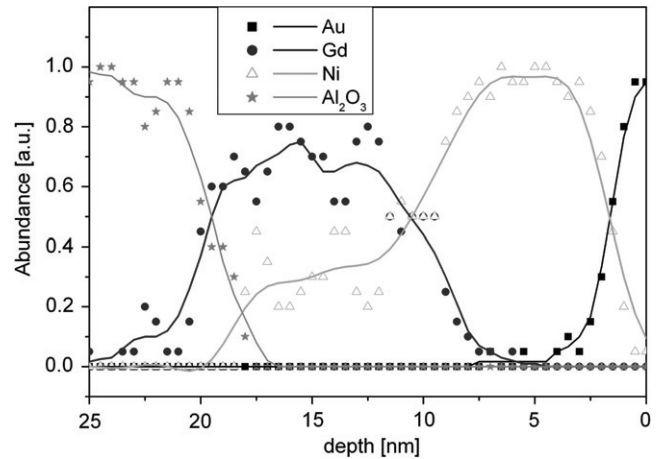


Figure 2. Depth profile of element distribution determined by RBS. Nominal sample composition is: $\text{Al}_2\text{O}_3/\text{Gd}(5.0 \text{ nm})/\text{Ni}(10 \text{ nm})/\text{Au}(2.0 \text{ nm})$ deposited at 100 K.

function of Ni layer thickness up to 10 nm. Then, Ni deposition was stopped and Gd deposition was started. There is a clear asymmetry in the saturation behavior for these two elements. In view of the rough Gd layer, it is suggested that Ni fills up the valleys until it forms a continuous Ni layer. At that point a rather flat Ni surface is produced, which was confirmed by STM measurements. Subsequent Gd deposition now leads to a fast saturation of the Gd AES signal within 1 nm. Note that such an asymmetric behavior could also be interpreted as alloy formation with a strong asymmetric diffusion character [11].

To further elucidate the interface structure, RBS experiments were performed. An elemental distribution as a function of depth is shown in figure 2. This was obtained by subsequently calculating RBS energy spectra from model configurations and comparison with the measured one. The symbols in figure 2 are the results of the simulation and the solid lines are averages between adjacent points and can only be taken as a guide to the eye. Again, a considerable overlap of Gd and Ni intensity is observed at the interface. This could be caused by alloy formation or, alternatively, could just come from the fact of a rough interface. Considering the observed Gd roughness by STM, which has the right magnitude to fully explain the AES and RBS data, we argue that alloy formation does not play a major role for our bilayers. Also, in the cases of Gd-Fe and Gd-Co film systems, little or no alloy formation was observed at the interface [16–19].

3. Magnetic characterization

Magnetic behavior was measured by a Quantum Design MPMS-5S XL SQUID magnetometer and element-specific XMCD, as discussed in section 4. A SQUID hysteresis loop measured at 45 K on the bilayer system $\text{Al}_2\text{O}_3/\text{Gd}(5.0 \text{ nm})/\text{Ni}(7.5 \text{ nm})/\text{Au}(2.0 \text{ nm})$, deposited at 100 K, is shown in figure 3. The applied external field for the loop is aligned parallel to the film plane. The arrows indicate the course of the loop, so one can see that the remanent moment is opposite to the previously applied external field ('negative remanence').

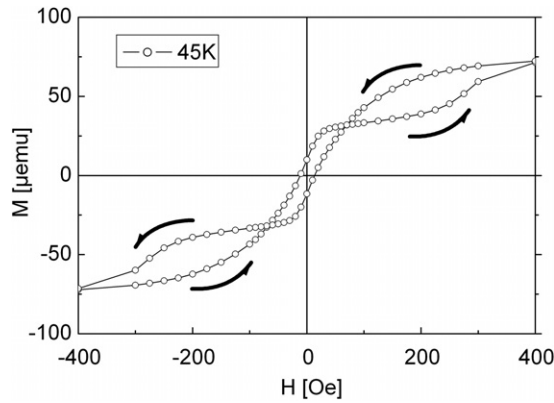


Figure 3. Hysteresis loop, recorded at $T = 45$ K, of a bilayer system $\text{Al}_2\text{O}_3/\text{Gd}(5.0 \text{ nm})/\text{Ni}(7.5 \text{ nm})/\text{Au}(2.0 \text{ nm})$ deposited at $T_{\text{dep}} = 100$ K.

At high fields both layers are magnetized parallel to the external field. Starting from high positive fields on the right-hand side of the graph in figure 3, we see the progression through the hysteresis loop in the so-called ‘Ni-aligned’ state. First, at saturation the magnetization of the Ni and Gd layers stays in the starting field direction. At an external field of about $+300$ Oe, the interlayer coupling field, favoring antiparallel alignment of Gd with the Ni moments, gradually switches the Gd layer magnetization. This antiparallel arrangement of Gd and Ni could now, in principle, align either with the Ni moments parallel to the external field or with the Gd moments along the external field. The higher Zeeman energy of the Ni layer given by the product of the coercive field and magnetic moment means that it takes more energy to switch the Ni than to switch the Gd, so the system remains Ni-aligned. In this ‘Ni-aligned’ situation, the high Gd moment overcompensates the Ni moment, leading to a negative remanence. Going to increasingly negative fields, the Ni magnetization finally switches, too, starting at about $H = -150$ Oe, and again both magnetizations are aligned parallel to the external field. The interlayer coupling observed in this hysteresis loop has been reported in other systems containing Gd and in other rare earth materials in contact with a magnetic transition metal [4, 5, 20–22].

The accurate temperature control of the SQUID magnetometer allows investigation of the temperature dependence of the magnetization. Hysteresis loops at different temperatures are shown in figure 4. The temperatures are 300 K, well above the Curie point of the Gd layer, 65 K, close above the Curie temperatures of the Gd layer on Al_2O_3 , and 45 K, where the Gd layer is ferromagnetic. At 300 and 65 K solely the Ni layer magnetization is observed. A strong increase of the coercivity field of the Ni film is visible, indicating a thermally activated magnetization process [23]. In contrast, at 45 K the Gd layer is now ferromagnetic, and antiferromagnetic interlayer coupling in the remanent state leads to the previously described negative remanence.

At lower temperatures the system switches to the ‘Gd-aligned’ state. Here the magnetic moment of the Gd layer follows the external field and the Ni moment aligns antiparallel

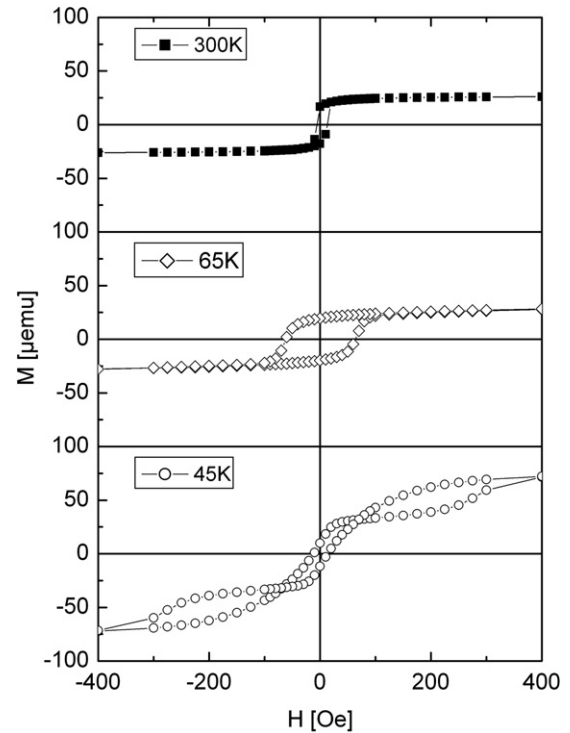


Figure 4. Hysteresis loops for three temperatures of the bilayer system $\text{Al}_2\text{O}_3/\text{Gd}(5.0 \text{ nm})/\text{Ni}(7.5 \text{ nm})/\text{Au}(2.0 \text{ nm})$ deposited at $T_{\text{dep}} = 100$ K for temperatures above the compensation point in the Ni-aligned state.

to it. This behavior can be seen in figure 5(a), showing hysteresis loops at 4 K. At this temperature the magnetic moment of the Gd layer is sufficiently large so that the moment of the Ni layer is now rotated due to the lower Zeeman energy at the presence of the antiferromagnetic interlayer coupling, as indicated by a rather broad field range between 2 and 5 kOe, where the external field gradually reorients the magnetic moment of the Ni layer. Note that the step height matches the saturation magnetization observed in the measurement at 300 K, confirming that the step is caused by the Ni moment. Figure 5(b) presents a close-up of figure 5(a) showing the switching behavior of the Gd layer, revealing a rather small coercivity of about 20 Oe.

The behavior seen in this series of hysteresis loops was investigated in more detail by recording the remanence (M_R) over temperature, shown in figure 6(a). The sample was saturated at each temperature point and the remanence was measured after turning off the external field. The measurements started at 300 K and the temperature was then reduced step by step. At temperatures above the T_C of Gd the remanence remains nearly constant, because T is far below T_C of Ni and, if magnetized along the easy axis, the ratio of remanence to saturation magnetization is nearly one. The remanence of the Gd/Ni bilayer deposited on $\text{Al}_2\text{O}_3(0001)$ only begins to decrease at temperatures below 60 K, indicating the appearance of a substantial moment of the Gd layer. The small sketches in figure 6(a) show schematically the magnetization directions of the remanent state of the bilayer system in the different temperature regions. At about 45 K we

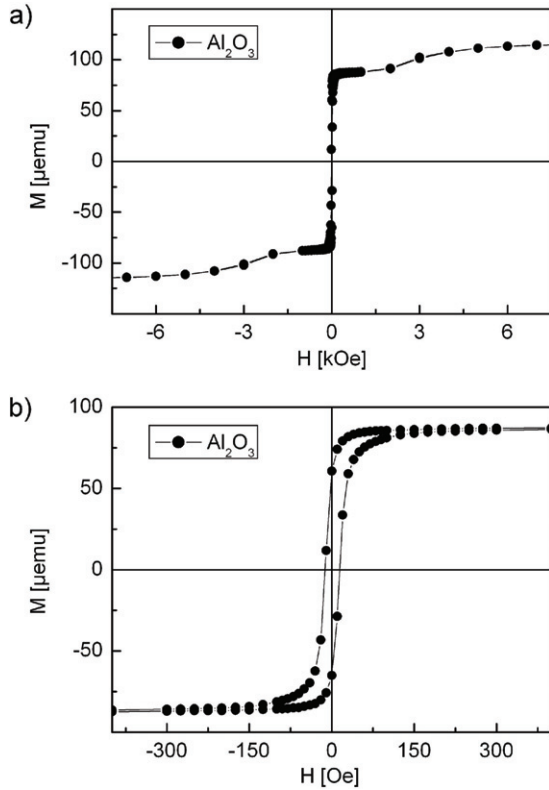


Figure 5. (a) Hysteresis loop in the Gd-aligned state, measured at $T = 4$ K. (b) shows a close-up of (a) revealing the switching process of the Gd layer.

see the point of maximum negative remanence. This point is also called the overcompensation point. At the compensation points where the Gd moments finally compensate the Ni moments the remanence is zero.

Figure 6(b) shows the saturation magnetization (M_S) in an external field of 10 kOe. The large diamagnetic contribution of the substrate was subtracted from the magnetization curves, leaving only M_S of the bilayers. The M_S values rise above the high temperature Ni baseline by decreasing the temperature somewhat below 100 K, indicating the onset of ferromagnetic order of Gd.

The magnetic behavior is slightly different for the Si_3N_4 substrate due to the different film growth characteristics (e.g. substrate and film roughness, as discussed above). As can be seen in figure 6(b), the Curie temperature for the Gd layer is higher on Si_3N_4 than on Al_2O_3 , and there is a wider temperature range of negative remanence on Si_3N_4 , while the overcompensation point remains about the same for these bilayer systems with the same Gd layer thickness. However, a much wider transition accompanied with an enhanced Curie temperature is observed on Si_3N_4 . Figure 7 shows the hysteresis curves at 45 K for Gd/Ni bilayers on the two different substrates. Note that the coercivity of Gd is greater on Si_3N_4 and its reversal behavior is sharper. In addition, the Ni layer switches at much higher fields on Al_2O_3 than on Si_3N_4 , 300 Oe instead of 180 Oe. The negative remanence is also larger on Si_3N_4 . These differences must be a consequence of the different growth morphologies of the bilayers on the two

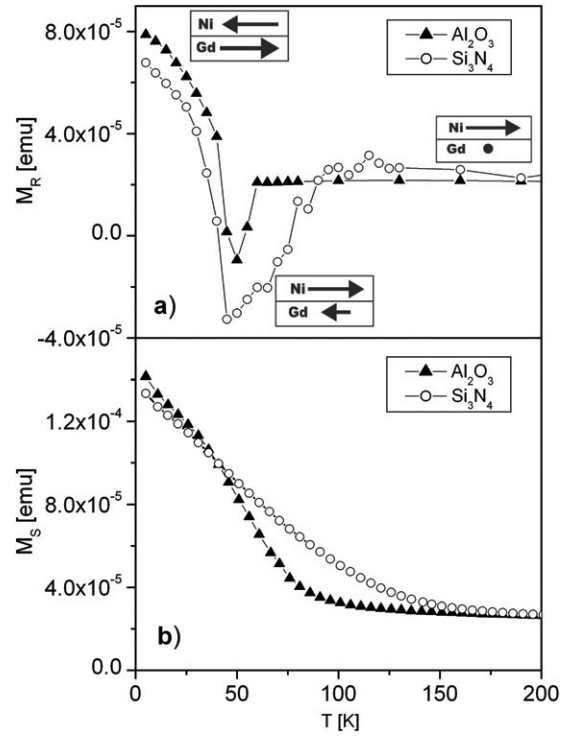


Figure 6. Temperature dependence of the magnetization of the bilayers Gd(5.0 nm)/Ni(7.5 nm)/Au(2.0 nm) deposited on Al_2O_3 and Si_3N_4 at 100 K: (a) the remanence after saturating the samples and switching off the external field; (b) the saturation magnetization at 10 kOe.

substrates, where the grain size and roughness of the Gd layer affect the observed magnetic properties. In this case a higher T_C on Si_3N_4 gives rise to a higher Gd magnetization on that substrate at a chosen temperature.

4. Element-specific XMCD measurements

In order to shed more light on the interlayer coupling, element-specific XMCD-measurements were performed on the bilayer system, $\text{Si}_3\text{N}_4/\text{Gd}(5.0 \text{ nm})/\text{Ni}(7.5 \text{ nm})/\text{Au}(2.0 \text{ nm})$. In the set-up used the sample holder and the magnetic field could be rotated separately with respect to the incoming beam. The rotation axes are perpendicular to the beam axis. This set-up allows the experimenter to keep the external magnetic field aligned in the plane of the magnetic layers, thus making it possible to compare element-specific in-plane hysteresis loops in transmission and reflection geometries. Measurements in transmission on the in-plane magnetized system Gd/Ni were carried out under an angle of 45° . So only the projection of \vec{M} on the incident beam \vec{k} is detected. This was necessary in order not to block the x-ray beam by the magnet pole in front of the CCD camera, which was fixed [24]. These measurements were performed on a membrane in the Si_3N_4 sample which was typically 150 nm thick. The transmission geometry detects the magnetization reversal of the individual layers independent of their depth, hence proportional to their corresponding magnetizations. In contrast, the reflection geometry yields a more surface-sensitive signal that can be

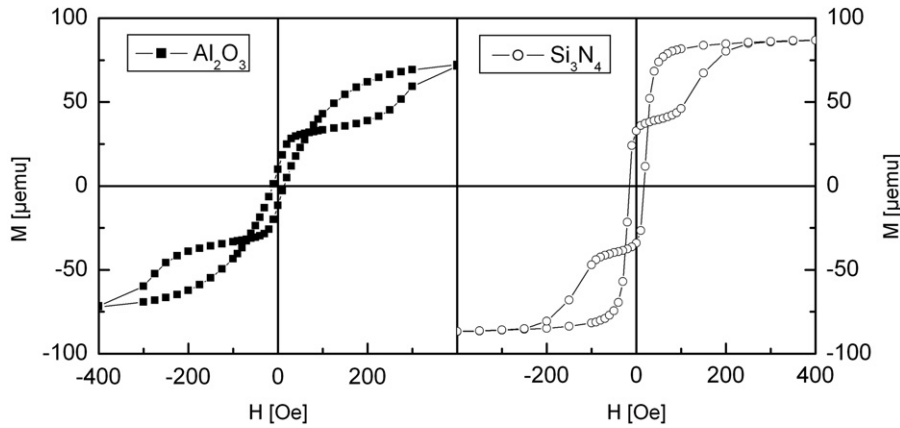


Figure 7. Hysteresis loops at the compensation point $T = 45$ K for bilayers deposited on Al_2O_3 (left) and Si_3N_4 (right) at 100 K.

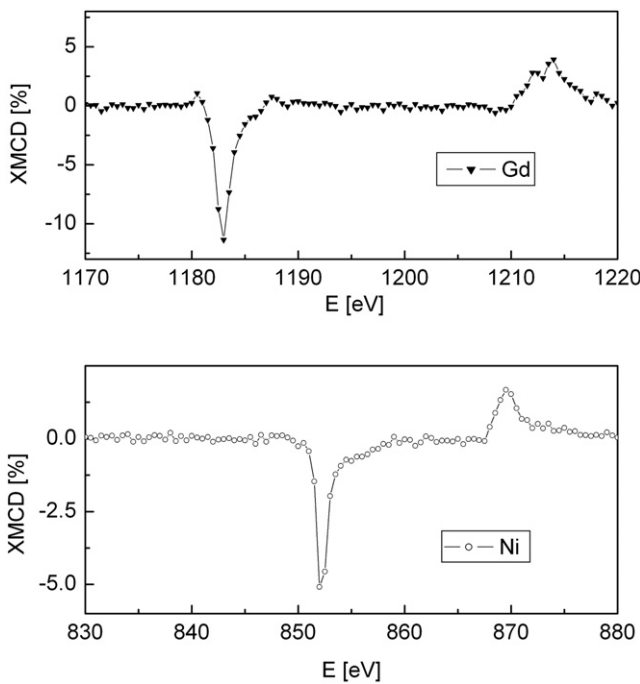


Figure 8. XMCD transmission spectra with absorption peaks at the $M_{4,5}$ edges for Gd and at the $L_{2,3}$ edges for Ni. The energy of the x-ray beam was changed in steps of 0.5 eV.

tuned towards a specific depth sensitivity via changing the incident angle as well as the energy across the corresponding absorption edge. The incident beam comes in at a small angle below 10° the XMCD signal is detected. The Gd/Ni bilayer XMCD transmission spectra are shown in figure 8. They were recorded at a temperature of approximately 60–70 K. The actual temperature had to be deduced from comparison with SQUID data, leaving an uncertainty of about ± 5 K. An XMCD signal of up to 10% can be obtained at the Gd M_5 edge ($E_\gamma = 1181$ eV) [25] and 5% at the Ni L_3 edge ($E_\gamma = 852$ eV).

Figures 9(a) and (b) show element-specific hysteresis loops for Gd and Ni, and a cartoon in figure 9(c) represents the magnetization directions for the layers at different points in the external field cycle. The vertical scales are different

between the two loops but within one measurement it gives a relative value of the magnetization of the respective layers. Starting from large positive fields at the positive saturation magnetization, we observe that most of the Gd switches at about +15 Oe, before remanence, revealing the antiferromagnetic coupling between the Gd and Ni layers, while some small residual portion of the Gd switches later at a reverse field of about -75 Oe. Interestingly, this small Gd portion exactly follows the magnetization direction of Ni during reversal but with opposite switching direction, indicating that the Gd magnetization direction is directly induced by the Ni layer with antiparallel alignment. Note that this induced moment corresponding approximately to one monolayer of Gd is even observed at room temperature, well above the Curie temperature of Gd in our system. This polarization of the interface layer of a rare earth by an adjacent magnetic transition metal is reported in the literature for many systems [7, 21, 26, 27]. Attempts to saturate the sample by applying fields of up to 5 T were not successful. Figure 9(b) shows a measurement at the Gd- M_5 edge in reflection geometry. XMCD reflection measurements, in contrast, show a much larger step at ± 75 Oe reverse field, indicating that at 10° incident angle the XMCD signal of this portion of the Gd is enhanced via charge/magnetic interference terms that dominate the reflected signal. Such magneto-optical interference can also affect the sign of the switching process as observed in figure 9(b). These results clearly demonstrate the simultaneous reversal of the Ni layer and the Gd moments at the interface at all accessible temperatures, even at 300 K, far above the Curie point of the thin Gd film.

The schematics in figure 9(c) help to clarify the magnetic evolution. It shows the magnetization directions of the individual layers, including a separate Gd interface layer which always remains antiparallel to the Ni layer magnetization.

5. Summary

Gd/Ni bilayer films were grown on Al_2O_3 and Si_3N_4 substrates at 100 K. While for both substrates an amorphous Gd film growth was observed, the Ni layer reveals a crystalline structure. However, intermixing between Ni and Gd could

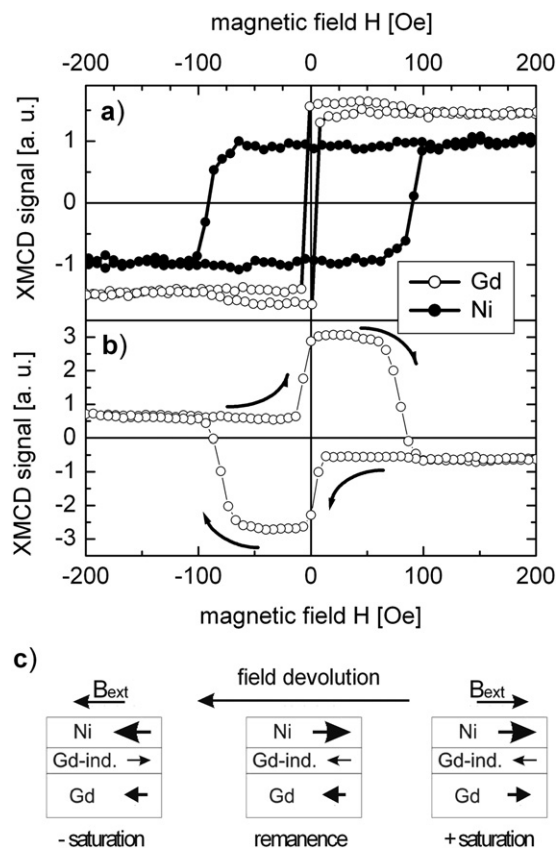


Figure 9. (a) Separate hysteresis loops for Gd and Ni, recorded in transmission. (b) XMCD in reflection at the Gd-M₅ edge, pronouncing the Gd interface moments. (c) Sketches of magnetization alignments for each layer.

not be ruled out from the structural studies. The magnetic investigation showed the interplay between the Ni and Gd bilayer where an antiferromagnetic interlayer coupling below the Curie temperature of Gd of about 100 K was obtained. The major magnetic effects, including hysteresis behavior, remanence and saturation magnetization, can be understood in terms of the different Curie temperatures of Gd and Ni, and their dependence on temperature. Moreover, element-specific XMCD studies revealed an additional magnetic Gd contribution which is induced by the Ni layer at the interface, which is always pointing antiparallel to the Ni magnetization and does not vanish even at room temperature. These results suggest that the formation of an additional NiGd alloy layer between Gd and Ni is not supported by these studies as an additional Ni contribution is not observed by XMCD.

Acknowledgments

Financial support by the Deutsche Forschungsgemeinschaft through the SFB 513 and the Emmy-Noether program are

gratefully acknowledged. The authors thank Andreas Liebig for early work on Gd evaporation in our laboratory, Professor H Hofsaess, University of Göttingen, for analysis of the RBS data, and Professor R R Vanfleet, Brigham Young University, Utah, for exploratory TEM experiments.

References

- [1] Baczewski L T, Kalinowski R and Wawro A 1998 *J. Magn. Magn. Mater.* **177–181** 1305
- [2] Koizumi A, Takagaki M, Suzuki M, Kawamura N and Sakai N 2000 *Phys. Rev. B* **61** 14909
- [3] Pogorily A, Shypila E and Alexander C 2005 *J. Magn. Magn. Mater.* **286** 493
- [4] Altuncevhahir B and Koymen A R 2001 *J. Appl. Phys.* **90** 2939
- [5] Altuncevhahir B and Koymen A R 2003 *J. Magn. Magn. Mater.* **261** 424
- [6] Colino J, Andres J P, Riveiro J M, Martinez J L, Prieto C and Sacedon J L 1999 *Phys. Rev. B* **60** 6678
- [7] Camley R E 1986 *Phys. Rev. B* **35** 3608
- [8] Haskel D, Choi Y, Lee D R, Lang J C, Srajer G, Jiang J S and Bader S D 2003 *J. Appl. Phys.* **93** 6507
- [9] Jensen J and Mackintosh A R 1991 *Rare Earth Magnetism* (Oxford: Oxford University Press)
- [10] Elliot R J 2005 *Magnetic Properties of Rare Earth Materials* (New York: Plenum)
- [11] LaGraffe D, Dowben P A and Onellion M 1990 *J. Vac. Sci. Technol.* **8** 2738
- [12] McGuire T R and Gambino R J 1978 *IEEE Trans. Magn.* **14** 838
- [13] Gonzales J A, Andres J P, Arranz M A, de la Torre M A L and Riveiro J M 2002 *J. Phys.: Condens. Matter* **14** 5061
- [14] LaGraffe D, Dowben P A and Onellion M 1989 *Phys. Rev. B* **40** 970
- [15] Pelka J B, Paszkowicz W, Wawro A, Baczewski L T and Seeck O 2001 *J. Alloys Compounds* **328** 253
- [16] Arnold C S, Pappas D P and Popov A P 1999 *Phys. Rev. Lett.* **83** 3305
- [17] Landes J, Sauer C, Kabius B and Zinn W 1991 *Phys. Rev. B* **44** 8342
- [18] Bertero G A, Hufnagel T C, Clemens B M and Sinclair R 1992 *J. Mater. Res.* **8** 771
- [19] Hosoito N, Hashizume H and Ishimatsu N 2002 *Japan. J. Appl. Phys.* **41** 1331
- [20] Ayres A M and Marinero E E 1996 *J. Appl. Phys.* **79** 5680
- [21] Takanashi K, Kurokawa H and Fujimori H 1993 *Appl. Phys. Lett.* **63** 1585
- [22] Cherifi K, Dufour C, Bauer P, Marchal G and Mangin P 1991 *Phys. Rev. B* **44** 7733
- [23] Skomski R 2003 *J. Phys.: Condens. Matter* **50** R841
- [24] Grabis J, Nefedov A and Zabel H 2003 *Rev. Sci. Instrum.* **74** 4048
- [25] Takagaki M, Koizumi A, Kawamura N, Suzuki M and Sakai N 2003 *J. Phys. Soc. Japan* **72** 245
- [26] Weller D, Alvarado S F, Gudat W, Schröder K and Campagna M 1985 *Phys. Rev. Lett.* **54** 1555
- [27] Ishimatsu N, Hashizume H, Hamada S, Hosoito N, Nelson C S, Venkataraman C T, Srajer G and Lang J C 1999 *Phys. Rev. B* **60** 9596